

CALIBRATION TARGET FOR ESTIMATION OF FREQUENCY DEPENDENCE IN SYNTHETIC APERTURE SONAR

Stig A V Synnes^{a,b}, Ole J Lorentzen^a

^a Norwegian Defence Research Establishment (FFI), PO Box 25, NO-2027 Kjeller, Norway.

^b University of Oslo (UiO), Department of Informatics PO Box 1080, Blindern, N-0316 Oslo, Norway.

Contact author: Stig A V Synnes,
Norwegian Defence Research Establishment (FFI), PO Box 25, NO-2027 Kjeller, Norway.
E-mail: Stig-Asle.Synnes@ffi.no

Abstract: *Synthetic aperture sonar (SAS) can provide high resolution images of the seafloor backscatter. A current research topic is whether wider bandwidth and lower frequencies can support better discrimination of different materials. In principle, the frequency dependence of the backscatter can be estimated at high resolution over the image. We suggest a calibration target that can provide simultaneous ground truth on both strength and frequency dependence of the backscatter.*

We develop an extended target consisting of objects with different combinations of scattering strength and frequency dependence. In order to provide deterministic frequency dependencies, we use solid geometrical shapes in the form of spheres, cylinders/cones and corners as reflectors. The scattering strengths of these reflectors are functions of frequency to the power of 0, 1 and 2, respectively. These three frequency dependencies are combined with different scattering strengths by using replicas of different sizes. We try to limit the acoustic footprint of the targets to a point where possible, in order to support processing at the maximum SAS resolution. We mount the objects on a metal plate, and elaborate on the choice of material and thickness needed to provide the required acoustic properties at the frequencies under investigation.

Finally, we present SAS images of a prototype target measured both at and outside of the design frequency. The suggested calibration target should be well suited to validate algorithms extracting the frequency dependence, and their ability to isolate the frequency dependence from the scattering strength.

1. INTRODUCTION

Synthetic aperture sonar (SAS) has become a major success for seafloor surveillance, providing high resolution images with large area coverage. Its applications are wide and include, but is not limited to, naval mine hunting, searching for wrecks, mapping of dumped WWII conventional and chemical munitions, underwater archeology, pipeline inspection and mapping for oil rig decommissioning [1–3].

A current trend in SAS research is to investigate the added value of wider bandwidth and lower frequency, as these have the potential of supporting better discrimination of different materials, thereby improving the performance for many applications [4].

At FFI we have been developing an algorithm to extract the frequency dependence of the scattering at high resolution over a SAS image. When testing the algorithm, we observed that the estimated frequency dependence increases with the estimated scattering strength. The correlation was not expected and could indicate an error in the algorithm. We therefore are in need of a calibration and validation target, that contains different combinations of scattering strength and its frequency derivative.

In this paper we develop a SAS target that allows for validating methods and algorithms designed to extract the frequency dependence of the acoustic scattering, and to isolate frequency dependence from scattering strength.

2. METHOD

We suggest and develop a calibration target consisting of reflectors with different combinations of frequency dependence and scattering strength. It would be hard to find materials with the same scattering strength or frequency dependence over a wide frequency area. We therefore opt for using targets of simple geometrical shapes that provide different frequency dependencies. In order to support high resolution SAS, we also choose scatterers with a single point acoustic footprint where possible.

We choose to arrange the reflectors in a matrix pattern, such that row number reflects the intensity and the column number reflects the frequency dependence. Thus the calibration target can be used to validate estimation of both intensity and frequency dependence, in the presence of variations on the other.

We choose to mount the targets on top of a smooth metal plate, that is thick enough that the reflection off the seafloor is minimal. This will make it possible to isolate also weaker scatterers, in contrast to mounting the targets on a frame where they would be observed on top of the seafloor scattering.

2.1 Frequency Dependent Scattering with Geometrical Shapes

In order to provide deterministic frequency dependencies, we use solid geometrical shapes in the form of spheres, cylinders/cones and corners as reflectors. The scattering strength of geometrical shapes can be estimated directly from the geometry when the target dimensions are much larger than the wavelength. At wavelength λ the target cross section is $\sigma = 4\pi A^2/\lambda^2$, where A is the effective area (of a flat plate with the same scattering strength) and the scattering strength in dB re 1m follows as $TS = 10 \log(\sigma/4\pi)$ [5, Sec 3.2].

We have examined the list of reflectors in [6] and focus on the few listed in Table 1. We observe that the scattering strength of these reflectors is a function of frequency to the power of 0, 1 and 2, depending on whether they are curved around two, one or no axes, respectively. Trihedrals provide single point acoustic footprint, as does the bicone when observed from its symmetry plane. The maximum scattering strengths for the shapes are listed in Table 1. For

simplicity of predicting the targets' scattering cross sections, we assume small grazing angles and choose targets of scattering strengths 0.01 m^2 , 0.1 m^2 and 1.0 m^2 .

Mirrored Shape	Scattering Cross Section
Half Sphere	πr^2
Cylinder	$4\pi r h^2 / \lambda$
Balancing Cone	$16\pi r^3 / (9\lambda)$
Triangular Trihedral	$8\pi h^4 / \lambda^2$

Table 1: Maximum scattering cross section σ for geometrical shapes mounted on a reflecting infinite plane and observed at low grazing angles. The arguments are target radius r and height h , and the acoustic wavelength λ . The frequency dependence follows from $\lambda = c/f$, with sound speed c and frequency f . The formulas were derived from [6, Chapter 6] and [7].

2.2 Plate Thickness

We would like the plate to provide a no-return area, masking the seafloor reflection, such that the object return is clean. This can be obtained by a low transmission through the plate for relevant seafloor grazing angles. For SAS, typical grazing angles are between 5 and 40 degrees.

Formulas for predicting the reflection and transmission off metal plates suspended in water are derived in [8]. For plates described through their dilational and shear wave speeds, along with density and thickness, sample predictions of reflection and transmission are showed in Fig. 1. For a given material, the prediction can be transferred to another sensing frequency

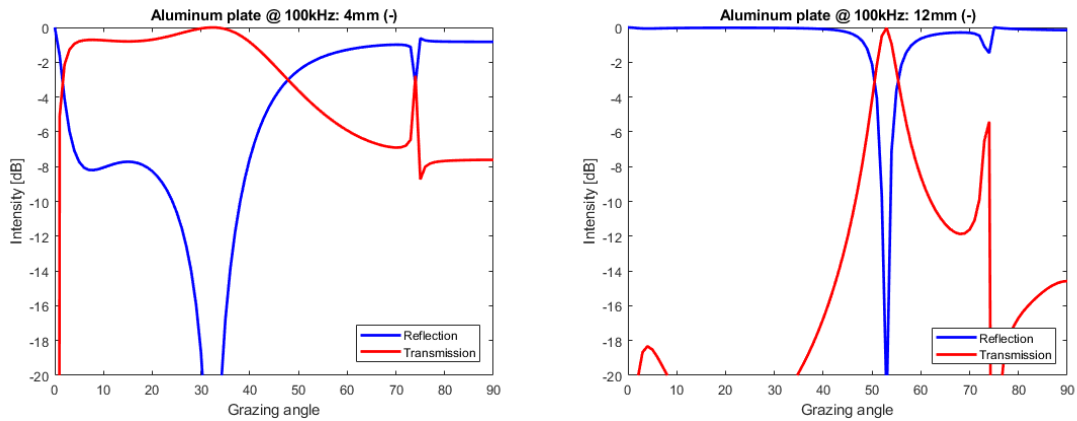


Fig. 1: Reflected and transmitted energy off 4 mm and 12 mm thick aluminum plates at 100 kHz, predicted from [8].

or plate thickness by keeping the product of frequency and thickness fixed. We find that for grazing angles below 30-40 degrees, aluminum plates provide *two-way transmission loss* at 100 kHz of around 2dB@4mm, 20dB@8mm, 40dB@12mm and 60dB@16mm plate thickness. For steel plates, the corresponding *two-way transmission loss* at 100 kHz is around 4dB@4mm, 20dB@6mm and 40dB@8mm. Steel has roughly three times the density of aluminum, with 7820 kg/m^3 versus 2700 kg/m^3 .

If we have strong reflection off the plane at near normal incidence, the bicone target can be simplified by using a single standing cone, mirrored on the plate. In order to construct the

trihedral corner reflector from plates, we depend on strong scattering for any incident angle. We observe that both for aluminum and for stainless steel, the intensity loss for the reflected signal at 100 kHz is smaller than 1 dB from grazing angles above 60 degrees. There is, however, a strong intensity loss around 45-55 degrees for both materials and most plate thicknesses. As a result, corners made of metal plates will not provide the desired scattering strength.

3. EXPERIMENTAL RESULTS

We present SAS images of a prototype calibration target that was made before our knowledge on plate reflection and transmission was gathered. This target was first measured in the spring of 2017 during FFI's MAREX'17 marine robotics exercise, using the HISAS 1032 SAS of FFI's HUGIN-HUS autonomous underwater vehicle (AUV). The system was operated with 30 kHz bandwidth around 100 kHz. After examining the results and observing that the target was barely visible, we acquired the mentioned knowledge on plate reflection and transmission, and found that our prototype should work more as intended at higher frequencies. At the time, Kongsberg Maritime was developing their new HISAS 2040 SAS for operation from their new MUNIN AUV and from the Hydroid REMUS 600 AUV [9]. During the testing of their first MUNIN AUV around the summer of 2018, Kongsberg Maritime accepted to both deploy our target and record a few lines past it. The onboard HISAS 2040 system operated with 60 kHz bandwidth around 250 kHz. However, as the deployment of the plate was challenging, we only have recordings of the plate upside-down and standing-on-the-edge. Though these data cannot be used for calibration, they still prove useful for evaluating the design of the prototype calibration target and as benchmark for the theory as reported here.

3.1 Prototype Calibration Target

We present a photo of our prototype target in Fig. 2. Note that this target was made before the knowledge on plate reflection and transmission was acquired, based on the assumption that the mounting plate would allow only minimal transmission. The target measures 1.8 by 1.2 m, and the mounting plate is made of 4 mm aluminum. The distance between objects with the same scattering cross section is 0.6 m, and the distance between lines of different scattering cross section is 0.3 m. The solid shapes are made of aluminum, and the trihedral corner reflectors of 1.5 mm acid-resistant steel. On the far right corner, there is a 35 cm long cylinder holding an acoustic transponder used for positioning.



Fig. 2: Photo of the prototype target before deployment. Photo: Kongsberg Maritime.

3.2 Measurements at 100 kHz

In the 100 kHz SAS images, the plate appears transparent, but the edges normal to the line of sight can be made out. With the geometry of the plate known, also the transponder position can be discriminated, and at low grazing angles also some of the stronger scatterers. It was confirmed by optical images that the target plate rests on a flat seafloor with the targets facing up.

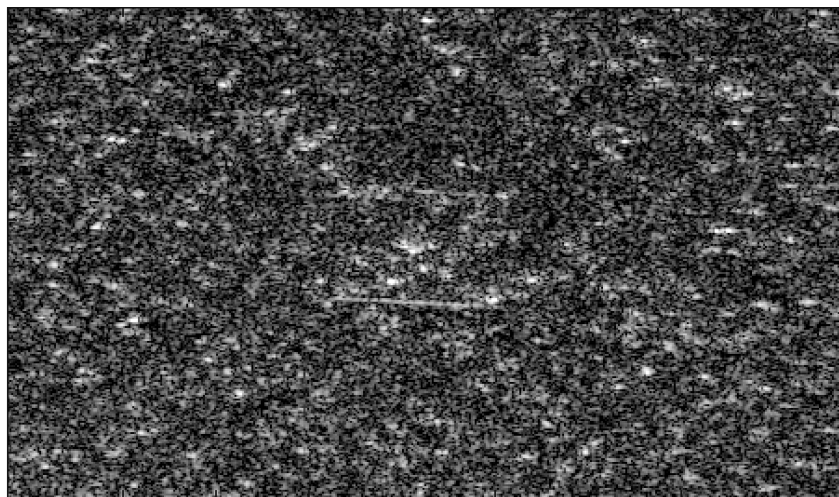


Fig. 3: SAS intensity image measured at 85-115 kHz with HISAS1032 from the HUGIN-HUS AUV. The image shows a 9 m x 5 m area covering plate and was recorded at 60 m distance and 10 m altitude.

3.3 Measurements at 250 kHz "upside-down"

The two SAS images of Fig. 4, recorded around 250 kHz from a HISAS 2040 on a MUNIN AUV, shows the target plate observed from two opposite directions. The images strongly indicate that the target plate is deployed upside-down, resting on the 35 cm long cylinder and the opposite short edge of the plate. The two SAS images shows the target plate observed from two opposite directions.

In the left image both the down-facing side of the plate with the reflectors and the seafloor beneath the plate are illuminated. The target intensities increase with the modeled target scattering strength. However, as the corner reflectors are illuminated normal to one of the cross-plates, a strong specular scattering occurs. Also, as the seafloor scattering is overlaid on the target scatterers, the weakest of the targets cannot be isolated from the background.

The right image shows the up-facing (rather smooth) back-side of the plate. The corner reflectors are clearly outlined, which is consistent with the fact that only these scatterers protrude through the plate. Some of the scatterers with low cross section are also more prominent than those of higher cross section, indicating that the target shapes closer to the edge could be partly insonified. We observe that there is a shadow beneath and behind the plate. The shadow is more filled-inn closer to the resting face of the plate.

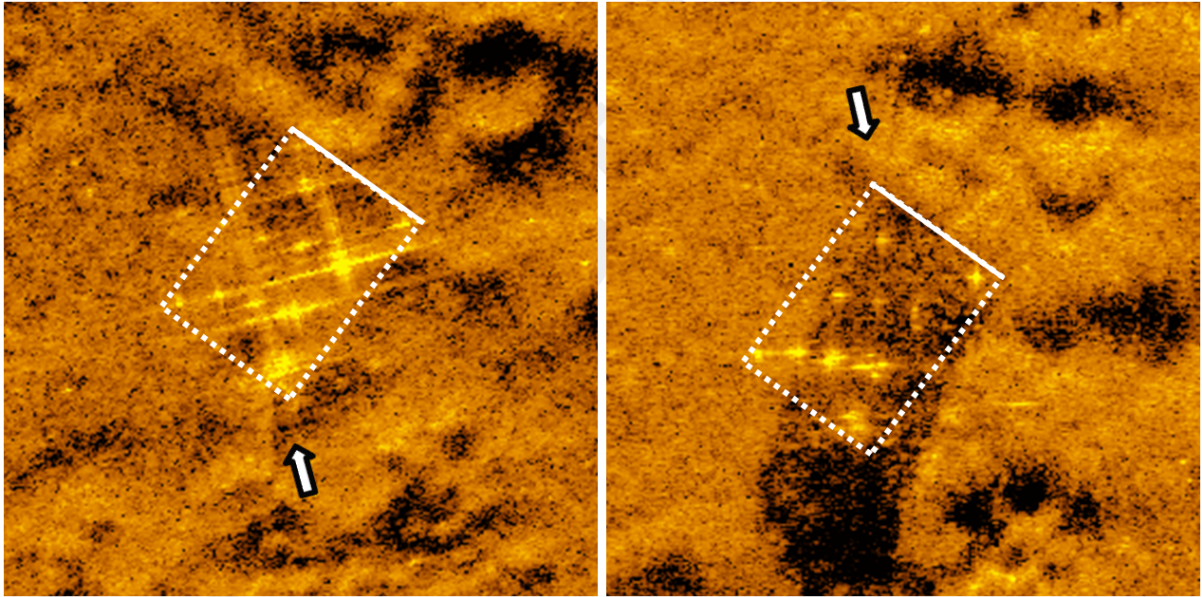


Fig. 4: SAS intensity images measured over 60 kHz around 250 kHz with HISAS 2040 from a MUNIN AUV. The two images are recorded from opposite directions at 33 m range and 4.5 m altitude, and the observation directions are indicated by white arrows. The plate appears to be resting upside-down, on a 35 cm long cylinder in the corner and on the opposite short edge of the plate. The outline of the plate is indicated by the white rectangle, and the solid line marks the edge resting on the bottom.

3.4 Measurements at 250 kHz "on-the-edge"

The two SAS images recorded around 250 kHz of Fig. 5 indicate that the target plate is deployed vertically, resting on the 35 cm long cylinder (holding an acoustic transponder) and its closest short edge of the plate. The two SAS images show the target plate observed from two opposite directions.

In the left image, the bottom side of the plate is illuminated at close to normal incidence. All the scattering is gathered on a short range-interval close to the resting face of the plate, and a high contrast shadow is observed behind the plate. (A junction between two images can be observed as an artefact on the left side of the scene.)

In the right image, the front side of the plate with reflectors is illuminated. Because of the vertical orientation of the plate, these are also gathered on a rather short range interval. Also here, a high contrast shadow is observed at some range behind the plate. However, at short range a seafloor is observed. This is in fact a mirror reflection of the seafloor in front of the plate, resulting from the top edge of the plate being closer to the sensor than the resting edge of the plate. Because of the opposite direction of observation, this patch resembles more a flipped cutout of the image with the opposite direction of observation.

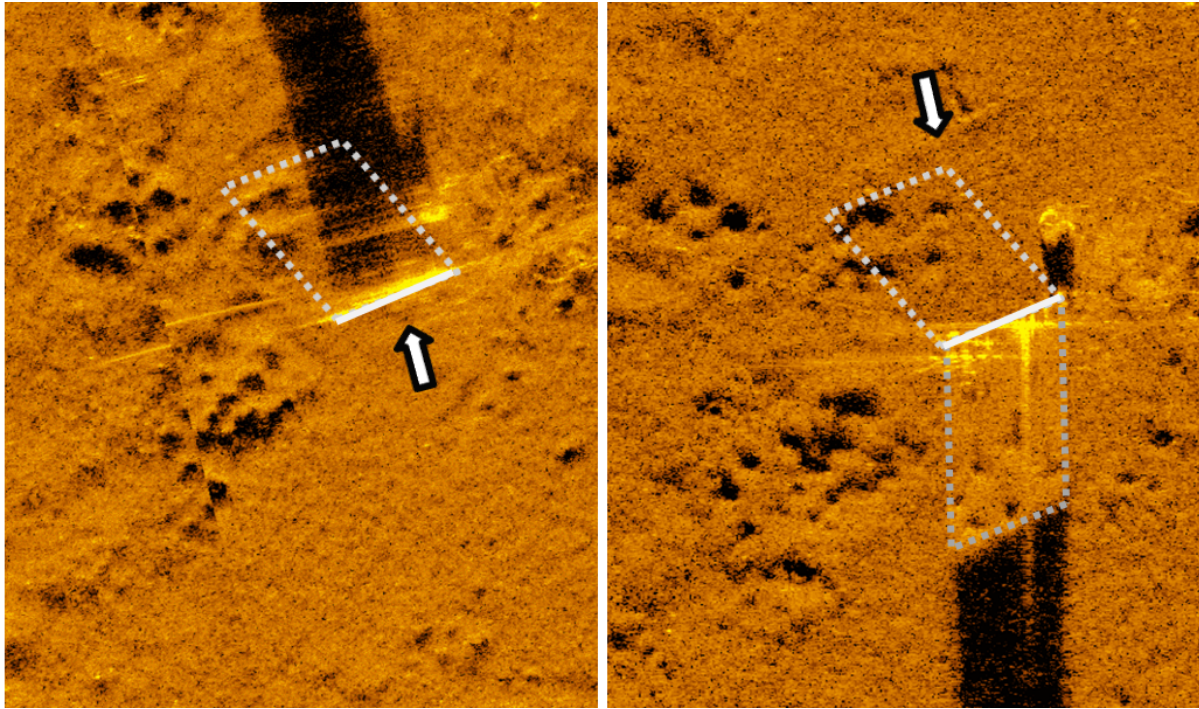


Fig. 5: SAS intensity images measured over 60 kHz around 250 kHz with HISAS 2040 from a MUNIN AUV. The two images are recorded from opposite directions at 33 m range and 5.0 m altitude, and the observation directions are indicated by white arrows. The plate appears to be resting vertically on a 35 cm long cylinder in the corner and on the closest short edge of the plate. The outline of the plate is indicated by the white trapezoid, and the solid line marks the edge resting on the bottom. The gray trapezoid indicates an area filled-in by mirroring off the plate.

4. DISCUSSION AND ANALYSIS

Our measurements of the prototype target shows that its mounting plate is transparent at 100 kHz, and that the attached reflectors are hard to separate from the seafloor. Our initial assumption that the 4 mm aluminum plate would not support transmission at 5-40 degrees grazing angles around 100 kHz was clearly wrong. After gathering the theory on scattering off metal plates in Section 2.2, these predictions confirm that the plate should provide only 2 dB reduction of the seafloor scattering at this frequency. However, the reduction of the seafloor scattering should rapidly increase if switching to a higher frequency. At 250 kHz the reduction should be around 30 dB, and this is qualitatively confirmed in Section 3.3. The targets are also strong compared to the background at 250 kHz, in contrast to what we experienced at 100 kHz, where our observations are consistent with the sound being transmitted through the plate, rather than reflecting off it. For normal incidence the theory indicates strong reflection, and indeed, with the vertically oriented plate of Section 3.4, we observe both a good image of the seafloor reflected off the plate, and a deep shadow.

In general, our measurements are in line with the predicted scatterings off both the aluminum plate and the targets. The prototype target has been useful as a benchmark for the theoretical models, but a redesign is needed for its intended use at 100 kHz: First, the mounting plate must be replaced by a 12 mm aluminum plate or a 8 mm steel plate in order to provide 40 dB

reduction of the seafloor scattering. Next, the trihedral reflector should get a solid backside, in place of being constructed from metal plates, as metal plates are predicted to give strong transmission for the important 40-50 degrees incidence angle of looking directly into the corner.

5. CONCLUSION

With the suggested changes, our calibrated target should be well suited for independent validation of scattering strength and frequency dependence estimates at 100 kHz. The target can be adapted for other frequencies by scaling the plate thickness and target dimensions inversely to the applied scaling of frequency.

ACKNOWLEDGMENTS

The authors wish to thank Georgia Tech and in particular Daniel A Cook for directing us to the theory for transmission and reflection off elastic plates. The authors also wish to thank FFI's Prototype Workshop and in particular Pål Halvorsen for producing refined drawings and building the prototype target based on our hand sketch. The authors wish to thank Kongsberg Maritime and in particular Terje Halvorsen for recording data on our test target as they were finalizing the first HISAS 2040 SAS system on the new MUNIN AUV. And furthermore, the authors wish to thank all the participants of MAREX'17, including the RNoN who provided optical underwater images of the target with their HUGIN-MR AUV. And finally the authors wish to thank our colleagues Roy E Hansen, Torstein O Sæbø and Marc Geilhufe in FFI's SAS-team for ever enthusiastic and inspiring discussions.

REFERENCES

- [1] Roy Edgar Hansen, Petter Lågstad, and Torstein Olsmo Sæbø. Search and monitoring of shipwreck and munitions dumpsites using HUGIN AUV with synthetic aperture sonar - technology study. Technical Report FFI-Rapport-19-00245, Norwegian Defence Research Establishment, 2019.
- [2] Øyvind Ødegård, Roy E. Hansen, Hanumant Singh, and Thijs J. Maarleveld. Archaeological use of Synthetic Aperture Sonar on deepwater wreck sites in Skagerrak. *Journal of Archaeological Science*, 89:1–13, 2018.
- [3] Arthur Ayres Neto, Geraldo Pinto Rodrigues, and Igor Drummond Alvarenga. Seabed Mapping with HISAS Sonar For Decommissioning Projects. *Sea Technology*, (September):15–18, 2017.
- [4] Roy Edgar Hansen. Synthetic Aperture Sonar Technology Review. *Marine Technology Society Journal*, 47(5):117–127, 2013.
- [5] Xavier Lurton. *An Introduction to Underwater Acoustics, Principles and Applications*. Springer, second edition, 2010.
- [6] Philip G. Gallman. *Radar Reflectors for Cruising Sailboats*. Ulyssian Publications, 2005.
- [7] Armin W. Doerry and Billy C. Brock. Radar cross section of triangular trihedral reflector with extended bottom plate. Technical Report SAND2009-2993, Sandia National Laboratories, 2009.
- [8] Ralph Fiorito, Walter Madigosky, and Herbert Überall. Resonance theory of acoustic waves interacting with an elastic plate. *J. Acoust. Soc. Am.*, 66(6):1857–1866, 1979.
- [9] *MUNIN AUV*, accessed April 11, 2019. <https://www.kongsberg.com/maritime/products/marine-robotics/autonomous-underwater-vehicles/AUV-munin/>.